

DUCTILITY DEGRADATION OF IRRADIATED FUEL CLADDING

A. Hermann, M. Martin, P. Pörschke, S. Yagnik¹⁾

¹⁾Electric Power Research Institute, Palo Alto, USA

The current trend in the nuclear industry towards higher fuel burnup is often accompanied by increased waterside corrosion and hydrogen pick-up of Zircaloy, contributing to its ductility degradation. Consequently, in the frame of the third phase of the Nuclear Fuel Industry Research (NFIR) Programme at PSI, work has been performed to evaluate the development of the decrease in ductility of Zircaloy-4 materials due to reactor irradiation and increasing hydrogen content. Tensile testing was applied to irradiated guide tube (GT) specimens, and the mechanical properties of the irradiated cladding were determined using burst-testing methods. The investigations have revealed a decrease in ductility of Zircaloy-4, mainly caused by irradiation, and only partly by increasing hydrogen content, but even after irradiation from a fast neutron fluence ($E > 0.82$ MeV) of ca. 10^{22} cm $^{-2}$, and a hydrogen pick-up of about 1000 wt.-ppm, an elongation of Zircaloy-4 cladding of $\geq 1\%$ was observed at high (≤ 350 °C), as well as at room, temperature. In contrast to elongation, the strength data remain nearly constant with increasing hydrogen concentration in the cladding metal.

1 INTRODUCTION

Increased waterside corrosion of Zircaloy under the harder operating regimes required to achieve higher burnups, and the higher degree of hydriding connected with it, could be a potential performance-limiting factor for nuclear power plants. Hence the need to investigate the mechanical properties of Zircaloy cladding at high burnups, to better understand the consequences for cladding integrity. In this context, many papers have been published on the influence of hydrides and/or irradiation on the mechanical properties of Zircaloy-4 (e. g. [1-6]). It was found that elongation of Zircaloy decreases with increasing hydrogen content, sometimes, depending on the kind of mechanical test, showing a ductile-brittle transition at a certain hydrogen level or test temperature [5-8]. But, only a few investigations of spent fuel rods have been performed, and these have focused on relating mechanical properties to burnup rather than giving detailed information on hydrogen content and distribution [9-12]. Consequently, a project within the NFIR programme has been undertaken at PSI to determine the decrease in ductility of Zircaloy-4 materials as a result of reactor irradiation and increasing hydrogen content.

Irradiated guide tubes and fuel rods (FRs) were included in the investigations. In parallel, a programme on non-irradiated (as-received and charged with hydrogen), archive Zircaloy-4 tubing samples, covering all metallurgical conditions, was procured to qualify the test methods and to obtain data for comparison.

Because of the close correspondence to in-reactor load, tensile tests were applied to guide tubes, and closed-end burst tests to fuel cladding. A variety of examination techniques were employed after the mechanical tests to obtain information on final deformation, fracture mode and hydrogen content, as well as distribution.

2 MATERIALS AND METHODS

2.1 Materials

Irradiated Ringhals-2 guide tubes (Zry-4, recrystallized) and four spent Goesgen Zry-4 fuel rods (2 stress-relieved, 1 late β -queched stress-relieved, and 1 recrystallized) were involved in the investigations. The sample material for the programme on non-irradiated archives was delivered by the NFIR group.

2.2 Methods

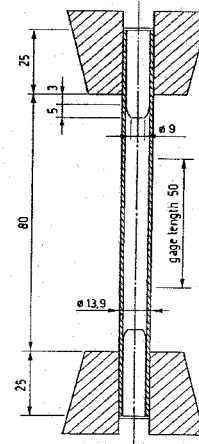


Fig. 1: Schematic view of a horizontal cut through the gripping jaws with a positioned GT specimen.

Tensile testing was applied to irradiated guide tube (GT) specimens comprising segments cut from the entire tubing (Fig. 1). The tests were performed using a fully computer-aided, servohydraulic MTS Material Test System with a 100 kN load frame, high temperature hydraulic wedge grips, an environmental chamber, and mechanical and optical strain gauges.

Closed-end burst testing with oil pressurization was performed on fuel cladding samples, after removing the fuel (fully or partly) using drilling procedures. The burst-test system was developed at PSI and placed within a shielded box.

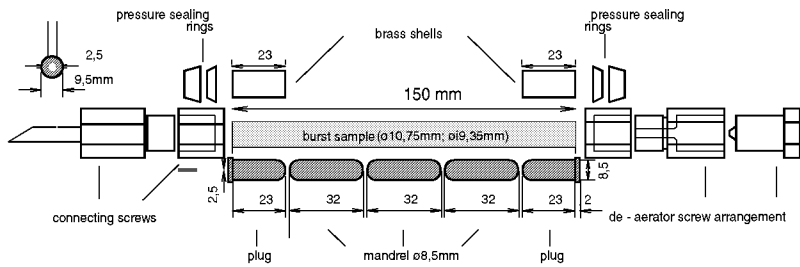


Fig. 2: Schematic of the sample mounting for burst testing.

The main components of the system are:

- a high pressure oil supply system allowing a linear pressure increase (0.01-1500 bar/s) up to rupture;
- a motor-driven, torque-wrench device for tightening the end seal caps; and
- a two-zone furnace placed below the bottom of the box, capable of accommodating the specimen together with the strain-measuring device (SMD);

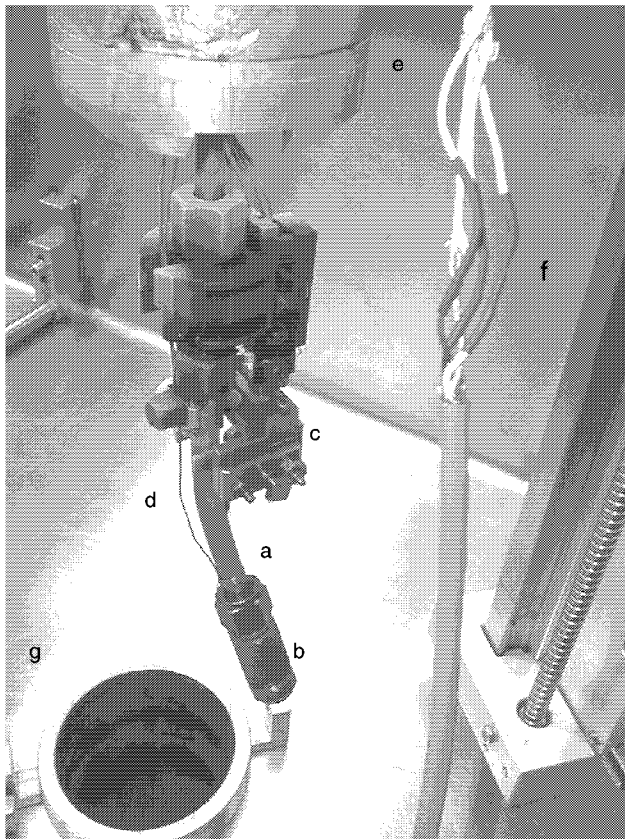


Fig. 3: View of the shielded box:

- a) sample after bursting; b) closed end; c) SMD; d) thermocouple; e) furnace cover; f) elevator for sample positioning; and g) furnace opening.

As illustrated in Figs. 2 and 3, the specimens were tightly closed at one end, and filled with steel mandrels (~8% clearance in diameter and length) to reduce the stored energy.

Figure 3 is a view into the burst box after a burst test and removal of the sample from the test position in the furnace. On top of the specimen, one can see the fixture of the SMD, which is based on an inductive displacement transducer capable of covering the entire temperature range from room temperature to 350°C. A high-precision, mechanical device transfers the movement of the probes to the piston of the transducer, as shown schematically in Fig. 4.

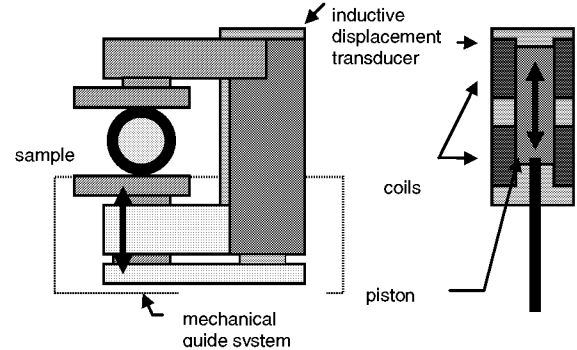


Fig. 4: Schematic of the strain-measuring device (SMD).

The plastic *Uniform Circumferential Elongation (UCE)* was determined from diameter measurements along the specimens before and after the burst test. The diameter was measured using a remote bench, in 5 mm steps, and along three straight axial lines of 60° at the cladding surface. The points of constant expansion, usually beginning at 2 cm distance from the burst opening, and covering 1-1.5 cm of the specimen length, were taken into consideration. The SMD could not be used because the position where the sample opens is not pre-determined. SMD was, however, used to determine the Young's modulus and 0.2% yield strength.

The plastic *Total Circumferential Elongation (TCE)* was determined by:

- wrapping a thin Al foil around the maximum bulge for non-irradiated samples; and by
- cutting a ring sample from the location of the maximum bulge, and by optical measurement of the circumference for irradiated samples. The section was mounted in cold-setting resin, and a polished metallography image was prepared. The computer code "analySIS", supplied by the company "Analysis", Muenster, Germany, and installed on a PC, was used for data evaluation (image analysis), and gave a relative reproducibility of about 1%.

The stress σ was calculated according to the formula:

$$\sigma = \frac{pD_i}{2t}$$

(p : pressure; D_i : inner tube diameter; t : wall thickness).

In the case of irradiated samples, for which direct measurements were impossible due to fuel and oxide, the inner diameter D_i and the wall thickness t were determined from the outer diameter D_o (measured before the test), taking into account (i.e. subtracting appropriately) the outside and inside oxide thicknesses (taken from the oxide thickness measurements before cutting, and from available metallography images), and the Pilling-Bedworth ratio (~2/3 of the oxide has to be related to the metal before oxidation). Also, the rod length increase during irradiation was measured for correction.

3 RESULTS AND INTERPRETATION

3.1 Tensile Testing on Guide Tube Material

Tensile tests were performed at room temperature and at 300°C on irradiated, as well as on non-irradiated (as-received and hydrogen-charged at GE¹ Vallecitos Nuclear Center), GT samples. The charging procedure resulted in some non-uniformity of the hydrogen distribution, and so the mechanical properties have been related to local hydrogen concentrations determined near the crack surface rather than to mean sample values.

The elongation data (elastic + plastic) of the non-irradiated samples are plotted against the local hydrogen content in the crack region in Fig. 5. The decrease of the total elongation with increasing hydrogen content is more pronounced compared with the uniform elongation. Whereas both uniform and total elongation at 300°C are represented by smooth curves in Fig. 5 at room temperature, uniform and total elongation are identical at hydrogen concentrations of about 1000 ppm and higher, giving an indication that from there on no necking occurs.

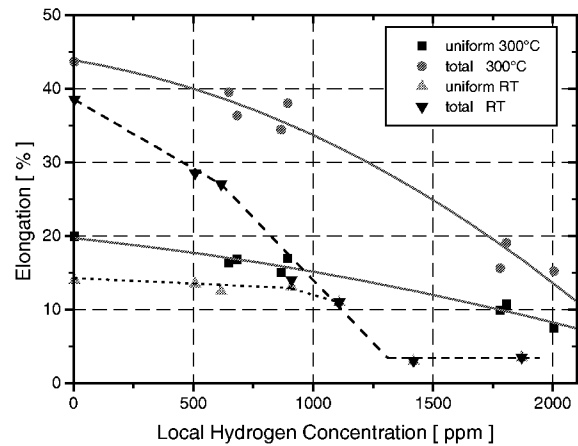


Fig. 5: Elongation of GT specimens as functions of hydrogen concentration.

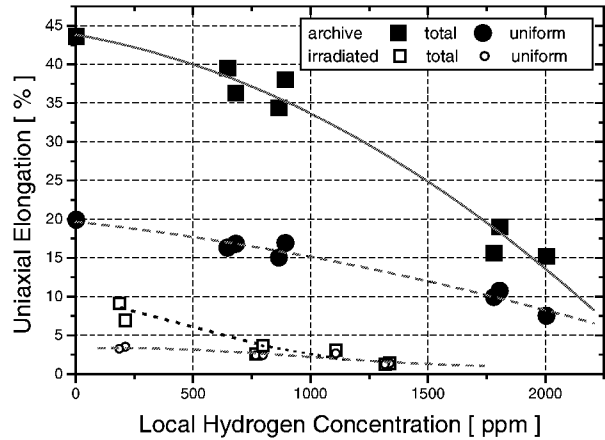


Fig. 6: Change of uniaxial elongation (elastic + plastic) with hydrogen concentration of neutron-irradiated ($\Phi: (7.7-8.2) \cdot 10^{21} \text{ cm}^{-2}$, $E > 0.82 \text{ MeV}$) and hydrogen-charged archive GT specimens at 300°C (strain rate $\sim 10^{-4} \text{ s}^{-1}$).

All data in Figs. 6 and 7 show a decrease in elongation with increasing hydrogen concentration. The drop in the elongation values from unirradiated to irradiated specimens at comparable hydrogen levels is considerable. The decrease in total elongation (ductility) caused by fast-neutron irradiation to a fluence of $7.7-8.2 \cdot 10^{21} \text{ cm}^{-2}$ ($E > 0.82 \text{ MeV}$) amounts to 80-85% at $\sim 250 \text{ ppm H}$ at room temperature and, at 300°C, the same relative decrease is observed up to a hydrogen level of $\sim 1100 \text{ ppm}$. Similar decreases in total elongation have been reported in the literature [13,14]. The disturbance for the development of slip systems in the deformation process coming from irradiation-induced obstacles (at the fluence investigated) seems more significant than that caused by hydrogen and hydrides. The irradiation damage is uniform, and causes the larger effect, since most of the hydrides are not concentrated in the fracture plane itself, but tend only to subdivide the metal into multiple layers.

¹ GE: General Electric

In contrast to elongation, increasing hydrogen content in samples has little influence on tensile strength: see Fig. 8, for example, in which considerable increase in strength due to irradiation is evident (irradiation hardening).

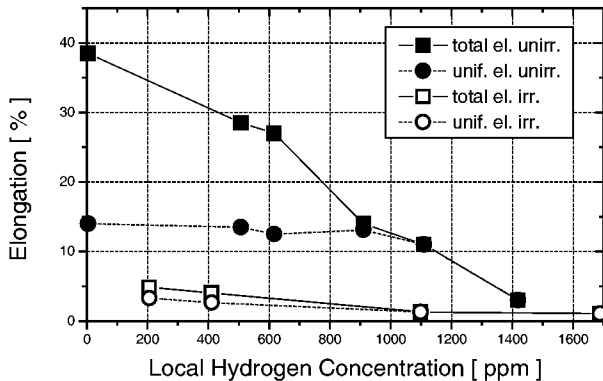


Fig. 7: Change of elongation (elastic + plastic) with hydrogen concentration of neutron-irradiated ($\Phi: 7.7\text{-}8.2 \cdot 10^{21} \text{ cm}^{-2}$, $E > 0.82 \text{ MeV}$) and hydrogen-charged archive GT specimens at room temperature (strain rate $\sim 10^{-4} \text{ s}^{-1}$).

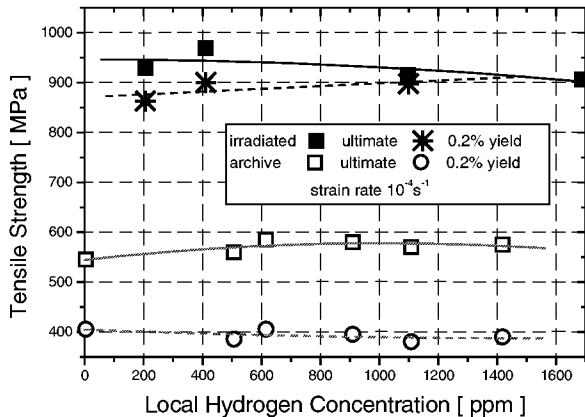


Fig. 8: Change of tensile strength with hydrogen concentration of fast ($E > 0.82 \text{ MeV}$) neutron irradiated ($\Phi: 7.7\text{-}8.2 \cdot 10^{21} \text{ cm}^{-2}$) and of charged with hydrogen archive GT specimens at room temperature.

3.2 Burst Testing on Fuel Cladding Material

Burst tests were performed at room temperature, 300°C, and 350°C, on irradiated, as well as on non-irradiated (as-received and hydrogen-charged at INER², Taiwan), fuel cladding (FC) samples. The SMD enabled us to record stress-strain data. As an example, results of burst tests at room temperature on archive samples, with different hydrogen content, are plotted in Fig. 9.

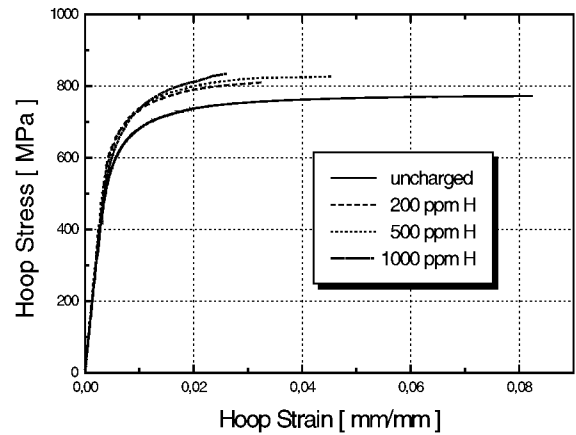


Fig. 9: Hoop stress-strain plots of burst tests at room temperature on stress-relieved FC samples with varying degrees of hydrogen charging.

Figure 10 shows the effect of hydrogen and irradiation on burst properties of stress-relief annealed (SRA) FC specimens. Most of the irradiated burst samples were of SRA initial metallurgical condition. Therefore, in Fig. 10, the data of the archive SRA series are plotted for comparison. Burst tests at 300°C and 350°C did not show differences within the experimental uncertainty, and are plotted together. At a hydrogen level of about 400 ppm, and at 350°C, the archive tubing shows a uniform circumferential elongation of 5-6% compared with about 1% elongation in fuel cladding irradiated to a fast-neutron fluence of $11 \cdot 10^{21} \text{ cm}^{-2}$ ($E > 0.82 \text{ MeV}$). At the same hydrogen level and temperature, the corresponding values for the total plastic circumferential elongation are $\sim 18\%$ and 2.8% , respectively. However, one should remember that the uniform distribution of hydrides in the archive tubing specimens is compared with the non-uniform hydride distribution in the irradiated FC samples (hydrides accumulated at the outer cladding wall).

The room temperature (RT) burst test results are shown in Fig. 11. The difference between irradiated and non-irradiated specimens containing more than ~ 400 ppm hydrogen is less pronounced at RT than at 300/350°C.

Comparing the data obtained from archive hydrogen-charged and irradiated specimens in Figs. 10 and 11, one concludes that the main contribution to the decrease in elongation (ductility) in the irradiated condition comes from fast-neutron irradiation, whereas the hydrogen accumulation adds only a little, if any, decrease. Nevertheless, a small further decrease in elongation with increasing hydrogen concentration can be noticed in the results with irradiated specimens, at least at 300/350°C. However the data are too scarce to be firm in this conclusion, and unfortunately the low hydrogen range is missing in the irradiated test series, where the steep decrease with increasing hydrogen concentration was found on archive specimens.

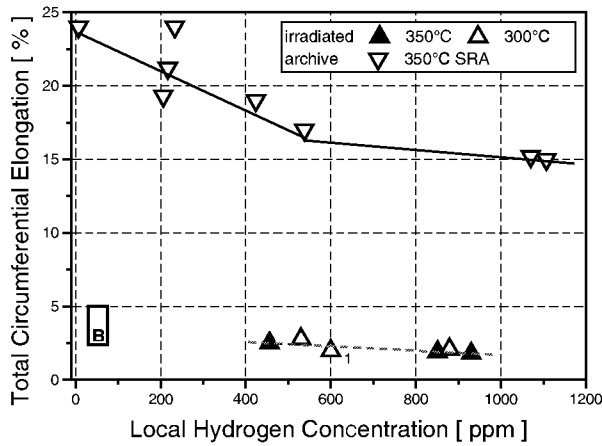
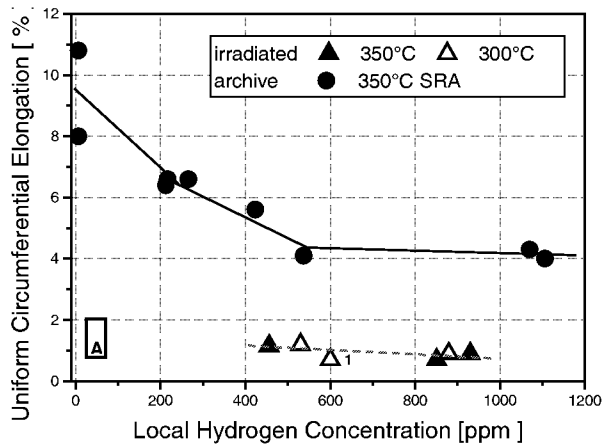


Fig. 10: Plastic uniform (A) and total (B) circumferential elongation of irradiated (fast neutron fluence $10-11 \cdot 10^{21} \text{ cm}^{-2}$, $E > 0.82 \text{ MeV}$) and archive stress-relieved FC samples with various degree of hydrogen charging at 300/350°C (¹late β-quench, strain rate $\sim 10^{-4} \text{ s}^{-1}$).

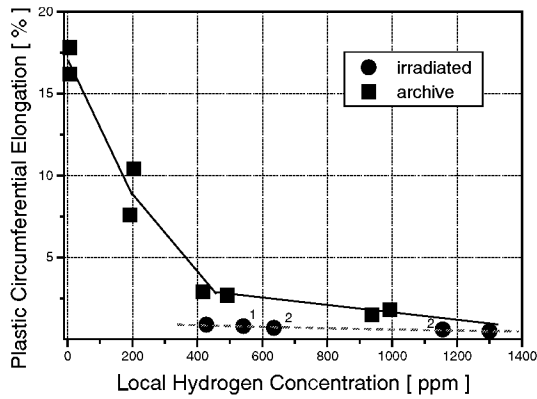


Fig. 11: Total plastic circumferential elongation of irradiated (fast neutron fluence $10-11 \cdot 10^{21} \text{ cm}^{-2}$, $E > 0.82 \text{ MeV}$) and archive stress-relieved FC samples, with various degrees of hydrogen charging, at RT (¹late β-quench, ²RXA).

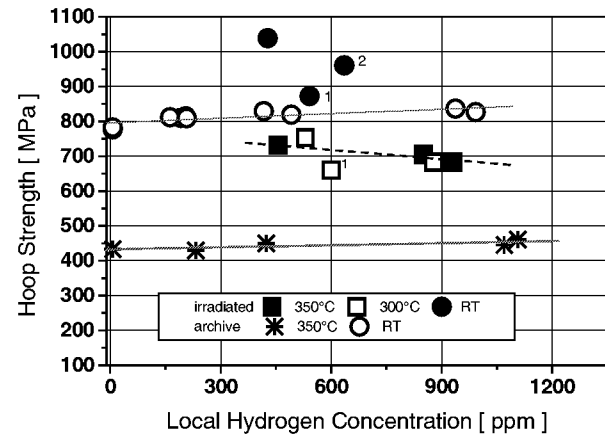


Fig. 12: Ultimate hoop strength of archive and irradiated stress-relieved FC samples with various degrees of hydrogen charging at RT and 300/350°C (¹late β-quench, ²RXA).

Concerning the dependence at room temperature (Fig. 11), one should remember that data on SRA, RXA, and late β-quenched SRA, are mixed in the irradiated data. Only the total circumferential elongation can be measured at RT because, in all cases, specimens ruptured with a long split over nearly the whole, free-sample length.

In Fig. 12, the burst strength of archive and irradiated FC specimens investigated in this project are compared. In tests at 350°C, the irradiation causes an increase in the ultimate hoop strength of nearly 100% (compared with the unirradiated case). In tests at room temperature, the neutron irradiation also leads to an increase in hoop strength, but the difference is smaller than at 350°C. From these data, an additional contribution of hydrogen to the hoop strength cannot be concluded with certainty.

3.3 Fracture Mode

With increasing hydrogen content in the archive tensile test series, the fracture mode at room temperature changes from ductile (ridges and void coalescence) in the uncharged specimens to moderate ductile (extended areas showing quasi-cleavage and an increasing number of microcracks caused by hydrides). With a magnifying lens it was established that through-wall fracture occurred $\sim 30^\circ-45^\circ$ to the load axis up to 600 ppm H, and normal to the load direction at higher hydrogen concentration. In contrast to the room temperature series at 300°C, a drastic change in the fracture behaviour occurs only at the 1800-2000 ppm level of hydrogen.

The fracture mode in tension of the irradiated GT samples is ductile in all cases, with increasing amounts of cracked brittle hydrides with increasing hydrogen content. Because of the many irradiation-induced obstacles disturbing the development of slip systems, localized deformation bands ($\sim 45^\circ$ to load direction), caused by dislocation channelling, can be observed if some degree of necking accompanies the final stage of deformation (e.g. [13], see Fig. 13, sample PGZ3).

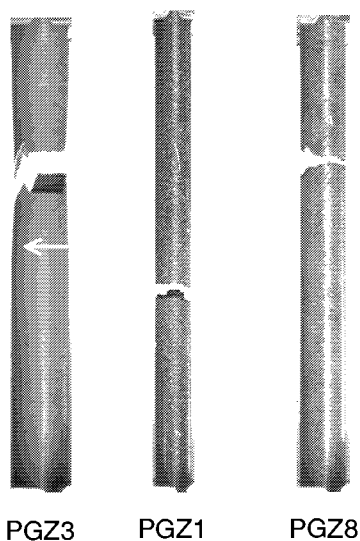


Fig. 13: Appearance of irradiated GT specimens after fracture at RT.

Specimens: PGZ3 (~205 ppm H)

PGZ1 (~550 ppm H)

PGZ8 (~1225 ppm H)

(dimensions are not exactly comparable)

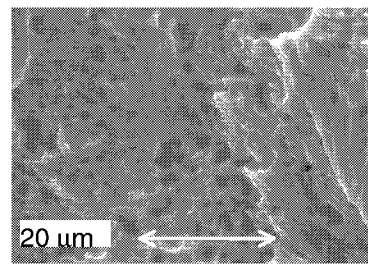
It is interesting to note that this behaviour, though to a much lesser extent, can also be assumed for the heavily hydrided non-irradiated GT specimens.

In the burst tests on archive samples at room temperature up to ~200 ppm hydrogen, the SRA samples failed in shear, with the shear plane lying at about 45° to the hoop stress direction. At higher hydrogen concentration (the next level investigated beyond the 200 ppm value was already ~500 ppm), the crack follows the radial direction, with some serration up to a certain depth, and continues with an ~45° shear plane. At 350/300°C, at all hydrogen levels, for SRA, late β -quenched SRA, as well as for RXA FC samples, failure occurs with ~45° shear.

The SEM images taken from the fracture surfaces after burst testing of irradiated samples reveal mostly ductile features. At low hydrogen concentration, there are minor differences between the tests at 350°C and at room temperature (see Fig. 14). With high hydrogen concentration, and at RT, microcracks are visible (see Fig. 15), but the signs of ductility are still present.

4 DISCUSSION

A comparison of the main burst test results on irradiated samples of this investigation with data from the literature can be made with the help of the compilation in Table 1. It is interesting to note that most burst-test results are published at temperatures $> 300^\circ\text{C}$, whereas only sparse RT data are available (see Table 1). From the literature data given in Table 1, the hydrogen content is given without further specification (e.g. average hydrogen content versus local accumulation at the burst opening). Therefore, for comparison purposes only, the values from this investigation are taken where local and mean hydrogen content are about equal.



A

Fig. 14: SEM images of the crack surface of the burst openings:

A: at 350°C

P5 (456 ppm H);

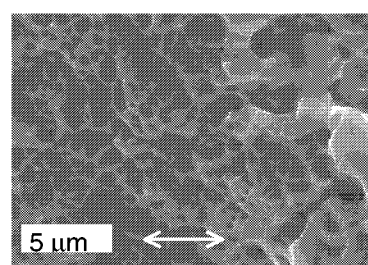
B: at RT

P4 (428 ppm H);

neutron fluence:

10^{22} cm^{-2}

($E > 0.82 \text{ MeV}$).



B

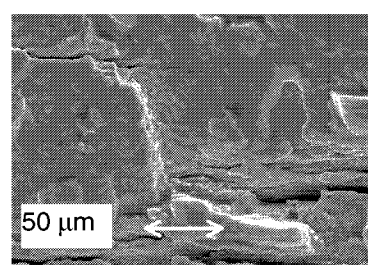


Fig. 15: SEM image of the crack surface of the burst opening: tested at RT P2 (1300 ppm H); neutron fluence: 10^{22} cm^{-2} ($E > 0.82 \text{ MeV}$).

A detailed investigation related to the hydride volume fraction in the outer third of the cladding, and its influence on the elongation results, is reported in [16]. This evaluation was not applied here, but could be included in a follow-up project. The value used in this investigation for relating mechanical test results to hydrogen content was the hydride concentration, determined from half of the cladding ring containing the crack opening. The metallography images available at PSI from PIE³ projects show variations in the densities of hydrides around the cladding circumference by a factor of up to 5. Because a hydride volume fraction can be determined only locally, it is difficult to specify a value which characterizes the entire specimen. Nevertheless, a comparison between both approaches should be performed in any follow-up project.

As can be seen from Table 1, our results are comparable with burst tests on the "Arkansas Nuclear One Unit 2" and "Calvert Cliffs Unit 1" fuel reported in [16]. Also, for Fort Calhoun fuel cladding, 2.15% plastic TCE at 315°C were published for a specimen with a hydrogen content of 400 ppm, and a neutron fluence of $11.6 \cdot 10^{21} \text{ cm}^{-2}$ ($E > 0.82 \text{ MeV}$) [12,13], comparable to our 2.8% (see Table 1).

Higher TCE values in the literature are related to lower fast neutron fluence levels, and to unknown hydrogen contents [17,18]. The UCE results of this investigation are between those published in [16] (1.49%, 2.11%, 2.11% and 0.77% at 315°C, 387-585 ppm H) and in [13] (0.05% at 315°C, 400 ppm H).

³ PIE: post irradiation examination

Table 1: Comparable results¹ of burst testing on irradiated Zircaloy-4 FC samples.

Source	Fast Neutron Fluence (10^{21} cm^{-2} , $E > 0.82 \text{ MeV}$)	Test Temperature [°C]	Hydrogen Content [ppm]	Ultimate Hoop Strength [MPa]	Plastic Circumferential Elongation [%]	
					uniform	total
this report	10-11	300/350	~500	753	1.2	2.8
this report	10-11	RT	428	1038		0.9
[11]ZN	~11	315	45-95			3 - 3.5
[15] ZN	15-16	315	120-170			0.8 - 2.7
[16]AN	11-12 ^a	315	289 320 336	860-1010	0.95 1.23 1.36	1.73 1.47 2.45
[16]CC	11-12 ^a	315	322 387 423 573 595	860-1010	2.6 1.49 2.11 2.11 0.77	3.30 5.04 2.41 2.22 3.16
[13]	11.6	315	400	793	0.05	2.15
[17]	~ 4-6 ^a	371	n.a.	640-680	2.3	3.9
[18]	6	350	n.a.	645	1.8-2.6	4.7-6.7

¹engineering values; n.a.: not analysed or announced; AN: Arkansas Nuclear One Unit 2; ZN: Zion; CC: Calvert Cliffs, Unit 1; ^a > 1 MeV.

For Fort Calhoun fuel cladding, an ultimate hoop strength of 793 MPa at 315°C was published for a specimen with a hydrogen content of 400 ppm, and a neutron fluence of $11.6 \cdot 10^{21} \text{ cm}^{-2}$ ($E > 0.82 \text{ MeV}$) [13]. This result should be compared with the the 753 MPa at 500 ppm H measured at 300°C in this investigation (see Table 1). Also, the strength values given in [16] are somewhat higher, but the lower test temperature should be considered.

All the results discussed above were achieved at strain rates near that used in our investigations: $\sim 10^{-4} \text{ s}^{-1}$.

The circumferential elongations measured in burst tests are plastic values. At room temperature, the Young's modulus was determined in burst tests to ~230 GPa. Using this modulus, the elastic hoop strain was evaluated to ~ 0.45% at 1000 MPa, and a total circumferential elongation at the burst point could be calculated taking into account the

small (if any) influence of hydrogen on the Young's modulus found in this investigation. Thus, the TCE (elastic and plastic) is > 1%, up to a local hydrogen content of ~ 1000 ppm, even at room temperature.

5 SUMMARY AND CONCLUSIONS

The objective of this project was to enhance understanding of the mechanical property changes, ductility and strength of LWR Zircaloy-4 fuel cladding at high burnups.

Tensile tests on tubing specimens of archive RXA guide tube material revealed a decrease in total elongation at RT from 38% to 3% with increase in H content from ~7 ppm to ~1700 ppm, at 300°C from 44% to 15%, in the H range from ~7 ppm to ~2000 ppm, and in uniform elongation at RT from 14% to 3%, at 300°C, from 20% to 7.5%, in the same hydrogen range as above.

Tensile tests on tubing specimens of irradiated Ringhals-2 RXA guide tube material, with fast ($E > 0.82$ MeV) neutron fluence Φ ($7.7 \cdot 8.2 \cdot 10^{21} \text{ cm}^{-2}$), revealed a decrease in total elongation at RT from 5% to 1%, with increase in hydrogen content from ~ 200 ppm to ~ 1700 ppm, and at 300°C from 9% to 1.3%, in the hydrogen range of ~ 190 ppm to ~ 1300 ppm, in uniform elongation at RT from 3.3% to 1%, and at 300°C from 3.5% to 1.3% (practically no difference to room temperature). Thus, the decrease in elongation (ductility) is mainly caused by neutron irradiation, and there is only a small additional contribution by increasing hydrogen precipitation.

The tensile strength of irradiated Ringhals-2 RXA guide tube material increases compared to archive samples with ~ 600 ppm hydrogen: with respect to the ultimate tensile strength at RT from ~ 580 MPa to ~ 950 MPa, and at 300°C from ~ 280 MPa to ~ 750 MPa, with respect to the 0.2% yield tensile strength at RT from ~ 400 MPa to ~ 900 MPa, and at 300°C from ~ 180 MPa to ~ 680 MPa. There is nearly no influence of hydrogen on tensile strength.

In burst tests on archive samples, the highest values of total plastic circumferential elongation were found on as-received RXA (56% [300°C], 28% [RT]), followed by late β -quenched SRA (41% [350°C], 23% [RT]) and SRA (24% [350°C], 17% [RT]) claddings. The same sequence is valid for the uniform circumferential elongation up to 600-800 ppm hydrogen content.

The total circumferential elongation measured in burst tests on irradiated FC specimens (Gösgen rods) is about 3% at 300°C and ~ 500 ppm H, and changes little with further increase in hydrogen content ($\sim 2\%$ at ~ 900 ppm H). At RT, TCE was found slightly above 1% at ~ 450 ppm H, and $\sim 1\%$ at ~ 1300 ppm H (local hydrogen near fracture). This means a decrease of the total plastic circumferential elongation by fast neutron irradiation at ~ 500 ppm H from 18% to 2.8% at $300/350^\circ\text{C}$, and from 2.7% to 0.9% at RT (compared to the SRA initial condition to which most samples belong). The data show that the decrease in ductility is mainly caused by neutron irradiation, and that the additional contribution by hydrogen in the cladding is relatively small.

The hoop strength of fuel rods irradiated in Gösgen increases compared to SRA archive specimens at ~ 500 ppm hydrogen: at RT from ~ 780 MPa to ~ 1040 MPa, and at 350°C from ~ 430 MPa to ~ 730 MPa, and the 0.2% yield hoop strength at 350°C from ~ 330 MPa to ~ 690 MPa. From these data, an additional contribution of hydrogen to the hoop strength cannot be concluded with certainty.

The remaining ductility of irradiated fuel rods (neutron fluence Φ : $10 \cdot 11 \cdot 10^{21} \text{ cm}^{-2}$, $E > 0.82$ MeV) can

be characterized as follows: at operating temperatures, and up to about 1000 ppm hydrogen, the total plastic circumferential elongation is still about 2% and higher, the uniform elongation $\geq 1\%$; at RT, the total plastic circumferential elongation is slightly below 1%, but the total elongation (plastic and elastic) which the cladding can withstand is about 1% and higher, up to hydrogen levels of ~ 1000 ppm.

ACKNOWLEDGMENTS

The authors would like to thank R. Brütsch for SEM investigations, Z. Kopajtic and M. Steinemann for hydrogen determinations, M. Gehringer and M. Sauder for metallography, H.-P. Linder, H. Schweikert and R. Zumsteg for sample preparation hotcell work, and G. Bart, R. Bühner, D. Gavillet and F. Gröschel for general support and valuable discussions. We are also indebted to B. Cox (University of Toronto) for suggestions in the interpretation of results.

REFERENCES

- [1] H.H. Burton, "Hydrogen Effects on Zircaloy-2 Tensile Properties", HW-61077 (1959).
- [2] D.G. Hardy, "The Effect of Neutron Irradiation on the Mechanical Properties of Zirconium Alloy Fuel Cladding in Uniaxial and Biaxial Tests", ASTM STP **484**, 215 (1970).
- [3] C.J. Baroch, "Effect of Irradiation at 130, 650, and 775°F on Tensile Properties of Zircaloy-4 at 70, 650, and 775°F", ASTM STP, **570**, 129 (1976).
- [4] J. Bai, C. Prioul, S. Lansiart, D. Francois, "Brittle Fracture Induced by Hydrides in Zircaloy-4", Scripta Metall. Mater., **25**, 2559 (1991).
- [5] J.-H. Huang, S.-P. Huang, "Effect of Hydrogen Contents on the Mechanical Properties of Zircaloy-4", J. Nucl. Mater., **208**, 166 (1994).
- [6] G.W. Parry, W. Evans, "Occurrence of Ductile Hydrides in Zircaloy-2", Nucleonics, **22**, 65 (1964).
- [7] J.-H. Huang, S.-P. Huang, C.-S. Ho, "The Ductile-Brittle Transition of a Zirconium Alloy due to Hydrogen", Scripta Metall. Mater., **28**, 1537 (1993).
- [8] A.A. Bauer, L.M. Lowry, "Tensile Properties and Annealing Characteristics of H. B. Robinson Spent Fuel Cladding", Nuclear Technology, **41**, 359 (1978).
- [9] M.G. Belfour, E. Roberts, E. DeQuidt, P. Blanc, "Zorita Research and Development Program: Final Report", WCAP-10180, Vol. 1, September 1982.

- [10] M.G. Belfour, W.R. Smalley, W.R. Kuszyk, P.A. Pritchett, "Hot Cell Examination of Zion Fuel - Cycles 1 Through 4", EP80-16, April 1985.
- [11] A.M. Garde, "Hot Cell Examination of Extended Burnup Fuel from Fort Calhoun", DOE/ET/34030-11 (1986).
- [12] A.M. Garde, "Effects of Irradiation and Hydriding on the Mechanical Properties of Zircaloy-4 at High Fluence", ASTM STP, **1023**, 548 (1989).
- [13] W. Evans, G.W. Parry, "The Deformation Behavior of Zircaloy-2 Containing Directionally Oriented Zirconium Hydride Precipitates", Electrochemical Technology, **4**, 225 (1966).
- [14] U.P. Nayak, H. Kunishi, W.R. Smalley, "Hot Cell Examination of Zion Fuel Cycle 5", EP80-16, June 1985.
- [15] A.M. Garde, G.P. Smith, R.C. Pirek, "Effects of Hydride Precipitate Localization and Neutron Fluence on the Ductility of Irradiated Zircaloy-4", ASTM STP, **1295**, 407 (1996).
- [16] L.M. Lowry, A.J. Markworth, J.S. Perrin, M.P. Landow, "Evaluating Strength and Ductility of Irradiated Zircaloy", BMI-2066, Vol. 1 (1981).
- [17] F. Garzarolli, R. Manzel, H. Schönfeld, E. Steinberg, "Influence of Final Annealing on Mechanical Properties of Zircaloy before and after Irradiation", Transactions of 6th SMIRT, Paris, August 17-21, 1981, Paper C2/1.